Electron Distribution and Molecular Motion in Crystalline Benzene: An Accurate Experimental Study Combining CCD X-ray Data on C_6H_6 with Multitemperature Neutron-Diffraction Results on C_6D_6

Hans-Beat Bürgi,[b] Silvia C. Capelli,[c] Andrés E. Goeta,[d] Judith A. K. Howard,[d] Mark A. Spackman,*[a] and Dmitrii S. Yufit[d]

Abstract: The electronic properties of the benzene molecule, for example its quadrupole moment and the electric field gradients (EFG's) at the H nuclei, are of fundamental importance in theoretical and experimental chemistry. With this in mind, single-crystal X-ray diffraction data on C_6H_6 were collected with a charge-coupled device detector at $T \approx 110$ K. As accurate modelling of the thermal motion in the crystal was regarded as vital, especially for the hydrogen atoms, anisotropic-displacement parameters (ADP's) for the C and H atoms in C_6H_6 were derived in a straightforward fashion from analysis of the temperature dependence of ADP's for the C and D atoms in C_6D_6 at 15 K and 123 K obtained by neutron diffraction. Agreement between C-atom ADP's derived from thermal-motion analysis of neutron data and those obtained from multipole refinement by using the X-ray data is extraordinarily good; this gives confidence in the modelling of vibrational motion for the H atoms. The molecular quadrupole moment derived from the total charge density of the molecule in the crystal is $(-29.7 \pm 2.4) \times 10^{-40}$ C m^2, in excellent agreement with measurements made in the gas phase and in solution. The average deuterium nuclear quadrupole coupling constant (DQCC) derived from EFG tensors at H atoms is 182 ± 17 kHz, also in excellent agreement with independent measurements. The strategy employed in this work may be of more general applicability for future accurate electron density studies.

Keywords: benzene · electric field gradient · isotope effects · quadrupole moment · X-ray diffraction

Introduction

Benzene is the prototypical aromatic molecule and, as such, assumes a role of central importance in the study of delocalized chemical bonds, of supramolecular interactions in the crystalline state and of chemical reactivity (either as a substrate or as a solvent). For this reason detailed knowledge of the numerous electronic properties of benzene and its closely related derivatives is of fundamental importance in many areas of theoretical and experimental chemistry. In this context it is an open question whether molecular properties of benzene, such as the molecular quadrupole moment and electric field gradients at H atoms (and hence deuterium quadrupole coupling tensors), can be obtained from modern X-ray diffraction data of charge density quality with an accuracy and precision comparable to that of other experimental results. The work described in this paper began with the explicit objective of answering that question. A good model of the molecular motions in the crystal, especially for the poorly scattering hydrogen atoms, is of paramount importance for determining accurate electron density distributions, but is not available from even the best X-ray-diffraction measurements. Given that neutron diffraction data at the same temperature as our X-ray experiment are not available, a substantial part of our study focuses on the derivation of reliable atomic displacement parameters (ADP's) of H atoms.

Although a number of outcomes from charge-density studies on crystalline benzene have appeared in various publications (see below), to our knowledge there has been no detailed experimental charge-density investigation of this key molecule. To date, all studies have been based on a rigid pseudoatom multipole model fitted to X-ray diffraction data

[a] Prof. M. A. Spackman
Chemistry, University of New England
Armidale NSW 2351 (Australia)
Fax: (+61) 2-6773-3268
E-mail: mspackma@metz.une.edu.au

[b] Prof. H.-B. Bürgi
Laboratorium für Kristallographie
Universität Bern, Bern (Switzerland)

[c] Dr. S. C. Capelli
Swiss–Norwegian Beamline
ESRF, Grenoble (France)

[d] Dr. A. E. Goeta, Prof. J. A. K. Howard, Dr. D. S. Yufit
Department of Chemistry, University of Durham
South Road, Durham, DH1 3LE (United Kingdom)

  0947-6539/02/0815-3512 $ 20.00+.50/0

collected on a CAD-4 diffractometer with Nb-filtered $Mo_{K\alpha}$ radiation on a single crystal of C_6D_6 grown in a capillary in situ at 123 K.[1] Positional and atomic displacement parameters of D atoms were taken from the careful neutron diffraction study on C_6D_6 at 15 K and 123 K by Jeffrey, Ruble, McMullan and Pople.[2] The published studies include those by Stewart[3] who reported maps of the molecular electrostatic potential and a topological analysis of the electron density, Spackman[4] who reported molecular second and quadrupole moments, Su and Coppens[5–7] who reported electrostatic potentials and electric field gradients at deuterium nuclei, and Brown and Spackman[8] who investigated in detail the determination of the electric field gradients at C and D nuclei. Unpublished work on the same data includes the original analysis by Jeffrey et al.,[1] which reported total and deformation electron densities, as well as analyses of the data appearing in theses by Goeta[9] and by Flensburg.[10]

Although Jeffrey et al. collected their X-ray data on C_6D_6 at 123 K to enable the use of neutron-derived positions and ADP's for deuterons, significant limitations have emerged in analyses of these X-ray data: carbon-atom ADP's determined from those X-ray data are systematically lower by 8–9% than the neutron values;[1, 8] this has a substantial effect ($\approx$20%) on estimates of the molecular quadrupole moment.[4] Blessing has described in detail a number of reasons why such discrepancies between neutron and X-ray ADP's are often observed for non-hydrogen atoms,[11] but it is clear that the uncertainties involved in any correction procedure would seriously compromise the objectives of our study. Although the X-ray data of Jeffrey et al. extends to $\sin\theta/\lambda = 1.18$ Å^{-1}, it is 99% complete out to 0.96 Å^{-1}, but only 71% complete overall; it is missing more than 60% of reflections in the range $0.96\,\text{Å}^{-1} < \sin\theta/\lambda < 1.18\,\text{Å}^{-1}$. Jeffrey et al. reported an internal agreement factor of 3.7%, and R factors after multipole refinements with that data have been reported in the range 3.1–5.4% (refinement on F) and 7.1% (refinement on F^2). For all of these reasons, the existing X-ray data were regarded as inadequate for a high-accuracy charge-density study, and it was decided to explore the quality of data that could be obtained with a modern CCD diffractometer.

Anisotropic displacement parameters: temperature dependence: ADP's are not available for C_6H_6, but have been measured by neutron diffraction on C_6D_6 at 15 and 123 K[2] and on the benzene complex $AgClO_4 \cdot C_6H_6$ at 18, 78 and 158 K.[12] In order to incorporate this information into the interpretation of the CCD X-ray data, two problems must be solved: 1) ADP's must be interpolated to the temperature of the CCD experiment, and 2) isotope effects must be taken into account. Both problems have been solved in the framework of a recently developed physical model of the temperature dependence of ADP's.[13]

The model describing the temperature dependence of ADP's is based on the assumption that the benzene molecule moves in the crystal field of its neighbours. The molecular motions are separated into a low-frequency and a high-frequency part (relative to the highest temperature of measurement). In the present case the former includes the molecular librations and translations, the latter includes the molecular deformations. They determine the ADP's, which are the diagonal 3×3 blocks of the more general atomic mean-square displacement matrix $\mathbf{\Sigma}^x$. This matrix, which also includes all correlations of motion of different atoms, is given by Equation (1):

$$\mathbf{\Sigma}^x = \mathbf{AgV}\delta(T)\mathbf{V}^T\mathbf{g}^T\mathbf{A}^T + \varepsilon = \mathbf{A}\begin{pmatrix}\mathbf{TS}\\ \mathbf{S}^T\mathbf{L}\end{pmatrix}\mathbf{A}^T + \varepsilon \quad (1)$$

Here $\mathbf{AgV}\delta(T)\mathbf{V}^T\mathbf{g}^T\mathbf{A}^T$ is an alternative representation of the T,L,S matrix of Schomaker and Trueblood,[14] showing the temperature dependence of T, L and S explicitly. The important quantities in this new way of expressing $\mathbf{\Sigma}^x$ are the elements of the diagonal matrix $\delta(T)$, which represent the mean square amplitudes of the low frequency librational and translational modes. According to the usual statistical thermodynamic expression [Eq. (2)]:

$$\delta_i(T) = \frac{\hbar}{2\omega_i}\coth\left(\frac{\hbar\omega_i}{2kT}\right) \quad (2)$$

The δ_i's depend on temperature, T, ω_i is a normal mode frequency, and k is the Boltzmann constant. $\mathbf{V}$, the eigenvector matrix, transforms the normal mode displacements to mass-weighted librational and translational displacements, $\mathbf{g}$ does the mass correction, and $\mathbf{A}$ makes the transformation from librational and translational to atomic displacements. Note also that $\mathbf{gg}^T$ is the Wilson matrix of reduced masses.[15] Finally, ε is the matrix of atomic mean-square amplitudes arising from the high-frequency intramolecular vibrations. Given that the lowest deformation frequency of benzene is about 300 cm^{-1}, ε is essentially temperature independent between the lowest and highest experimental temperatures.

The elements of $\mathbf{V}$, the frequencies ω_i and the diagonal 3×3 blocks of ε for carbon and deuterium atoms have been obtained by a least-squares calculation from the ADP's of C_6D_6 determined experimentally at 15 and 123 K, and have been given elsewhere.[16] The matrices $\mathbf{A}$ and $\mathbf{g}$ are straightforward functions of the atomic masses and the molecular coordinates chosen to describe the problem. Given the explicit temperature dependence of $\delta(T)$, the atomic mean-square displacements arising from libration and translation are easily calculated at any desired temperature.

Anisotropic displacement parameters; isotope effects: Isotope effects on the low frequency vibrations are treated within the same framework. At the high temperature limit, the product $\mathbf{gV}\delta(T)\mathbf{V}^T\mathbf{g}^T$ is the inverse of an analogous relation [Eq. (3)] used in normal mode analysis of vibrational spectra:

$$\lambda = \mathbf{gVFV}^T\mathbf{g}^T \quad (3)$$

Here λ is a diagonal matrix with elements ω_i^2 and $\mathbf{F}$ is a force-constant matrix. As usual, it is assumed that $\mathbf{F}$ is the same for all isotopomers. It is obtained from $\mathbf{g}_D$, $\mathbf{V}_D$ and λ_D determined above for the deuterated compound. With $\mathbf{F}$ and $\mathbf{g}_H$, the quantities $\mathbf{V}_H$, λ_H, $\delta_H(T)$ and, thus, the temperature-dependent part of $\mathbf{\Sigma}^x_H$ may be calculated for the protonated isotopomer.

  0947-6539/02/0815-3513 $ 20.00+.50/0

The analysis described in the preceding section also yields the mean-square amplitudes ε_D describing the effect of molecular deformations on C and D. Because there is no explicit mass dependence of ε_D and because the isotope effects on this quantity are more complicated, the corresponding ε_H cannot be obtained directly. Instead normal-mode analysis was performed on the ADP's of $AgClO_4 \cdot C_6H_6$ at 18, 78 and 158 K.[12] As the bond lengths and angles are very similar to those of C_6D_6, it was assumed that the intramolecular mean-square amplitudes of benzene in the silver complex are a good estimate of ε_H in benzene itself.

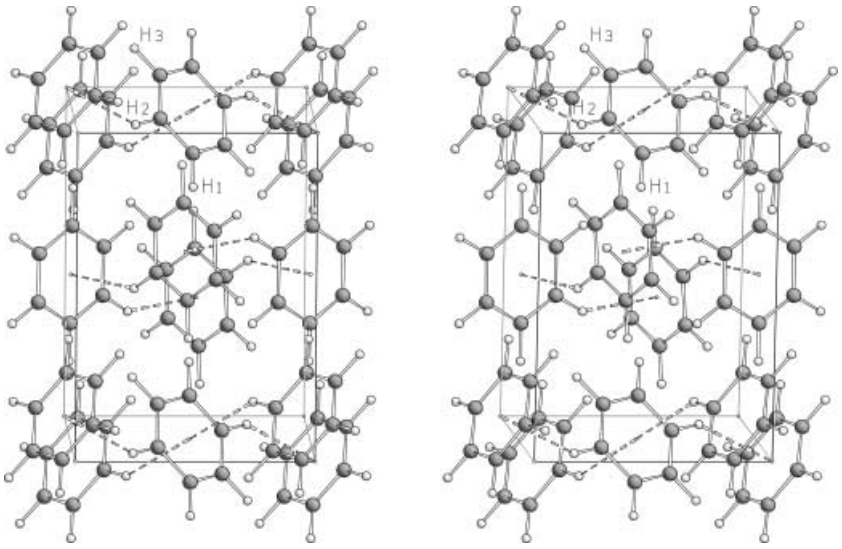

Figure 1. Stereo representation of the unit cell contents of benzene.[47] Note the close C–H$\cdots\pi$ contacts between H2 and adjoining benzene rings (indicated by dashed lines).

The elements of ε_H for C and H may also be estimated from force constants determined from spectroscopic normal-mode analysis or from high-level ab initio calculations on C_6H_6 in the gas phase.[17] Table 1 lists intramolecular mean-square amplitudes for C and H atoms from the neutron diffraction experiments on $AgClO_4 \cdot C_6H_6$ and from a spectroscopic harmonic force field that reproduces experimental infrared and Raman data.[17] The components along the C–H bond (ε_{11}) and in the molecular plane (ε_{22}) agree well, whereas the out-of-plane component (ε_{33}) is significantly smaller in solid $AgClO_4 \cdot C_6H_6$ than in gaseous C_6H_6. The ε's for C_6D_6 show similar behaviour and are given in Table 1 for comparison. The neutron diffraction and spectroscopic ε_H tensors for C_6H_6 are used in the subsequent multipole refinements.

Table 1. Intramolecular mean-square amplitudes (ε tensors $\times 10^4$ Å^2) for C and H/D atoms in C_6H_6 and C_6D_6. ε_{11} is along the C–H/D bond, ε_{22} in the molecular plane and ε_{33} perpendicular to the benzene plane.

	C atom			H/D atom		
	ε_{11}	ε_{22}	ε_{33}	ε_{11}	ε_{22}	ε_{33}
C_6H_6						
neutron diffraction[a]	14(1)	11(1)	11(1)	68(2)	124(2)	171(3)
spectroscopic force field[b]	9	12	14	61	130	202
C_6D_6						
neutron diffraction[c]	14(1)	7(1)	15(1)	52(1)	83(1)	110(2)
spectroscopic force field[b]	13	8	16	44	89	133

[a] From ADP analysis of neutron diffraction data for $AgClO_4 \cdot C_6H_6$[46] (the trace of ε(diffraction) was constrained to equal the trace of ε(spectroscopic)). [b] From an empirical force field based on estimated harmonic frequencies in the gas phase[17] (for details see Capelli et al.[16]). [c] From ADP analysis of neutron diffraction data for C_6D_6[2] (for details see Capelli et al.[16]).

Multipole refinements: A unit-cell diagram of the crystal structure is reproduced in Figure 1. The mid-point of each benzene ring is an inversion centre; this results in three unique C atoms and three unique H atoms. The rigid pseudoatom model for multipole refinement with X-ray diffraction data is well established, and a detailed description can be found elsewhere (see, for example, the excellent book by Coppens,[18] or Appendix A of Flensburg, Larsen and Stewart[19]). The modelling procedure seeks to derive an analytical representation of the electron distribution in the crystal, deconvoluted from the thermal motion of the atoms, by least-squares fitting to X-ray structure factors. The precise model chosen for fitting the benzene data in this work is for the most part quite standard, but it deserves to be described here in some detail as it is more extended and more flexible than is usually the case for molecular crystals. The multipole expansion extended up to the hexadecapole level for carbon atoms, and up to the quadrupole level for hydrogens (the latter is essential for a proper description of the deformations of quadrupole symmetry about the H atoms). No symmetry was imposed on any of the pseudoatoms. Core and spherical valence-electron densities of carbon atoms were constructed from products of localized atomic orbitals[20] based on the Clementi–Roetti atomic wave functions;[21] coefficients and exponents of these radial functions have been reported by Flensburg et al.[19] All other radial functions were of single exponential form, $r^n \exp(-\alpha r)$, with $n = 2,2,3,4$ (dipole through hexadecapole) for C atoms and $n = 0,1,2$ (monopole through quadrupole) for H atoms. The C-atom core populations were constrained to be equal; the valence monopole populations on C and H atoms were refined with the constraint that their sum equalled 5.0 electrons; all other population coefficients were varied freely. In addition, radial expansion/contraction of the valence monopole on carbon atoms was described by a single parameter, κ_C, all higher multipole radial functions on C atoms shared a single radial exponent, α_C, and all radial functions on H atoms shared a common exponent, α_H. Position parameters for all atoms were fixed at those obtained from neutron data at 123 K.[2]

Refinement strategy: From $\mathbf{V}_H$, $\delta_H(T)$ and ε_H, ADP's for C and H atoms in crystalline C_6H_6 were calculated between 100 and 114 K in steps of 1 K by using both "spectroscopic" and "diffraction" ε's (Table 1); this resulted in 30 different sets of

  0947-6539/02/0815-3514 $ 20.00+.50/0 *Chem. Eur. J.* **2002**, *8*, No. 15

calculated ADP's. A refinement strategy incorporating two related models has been pursued:

- Model A: multipole refinements were carried out by fixing the ADP's for C and H atoms at the 30 sets of calculated values;
- Model B: the ADP's of H atoms were fixed at the values calculated for the temperature that yielded the lowest R factor with model A, while the ADP's of C atoms were allowed to refine.

The more flexible multipole model (i.e. B) consisted of 18 ADP parameters, 98 population coefficients and 3 radial parameters, a total of 119 variables. All refinements and property calculations were carried out with the VALRAY set of programs,[22] based on 1766 reflections with $F_{obs} > 4\sigma(F_{obs})$, and minimizing the residual $\mathbf{\Sigma_H} w_{\mathbf{H}}(|F_{obs}(\mathbf{H})| - |F_{cal}(\mathbf{H})|)^2$, with $w_{\mathbf{H}} = \sigma^{-2}(F_{obs}(\mathbf{H}))$. The rather conservative 4σ cut-off on F is equivalent to a 2σ cut-off on F^2 (or I), and this was employed in order to obtain the most significant results possible. This is not uncommon in charge density analysis, especially where scattering includes a capillary as well as the sample. Moreover, because of the high completeness of the data collected, the ratio of observations to variables in the final multipole model (14.8) remains acceptably high even with this data cut-off.

Temperature of diffraction measurement: For model A, the lowest R values were found at $T = 110$ K for both sets of ε's (Figure 2), and the fits obtained by using diffraction ε's are

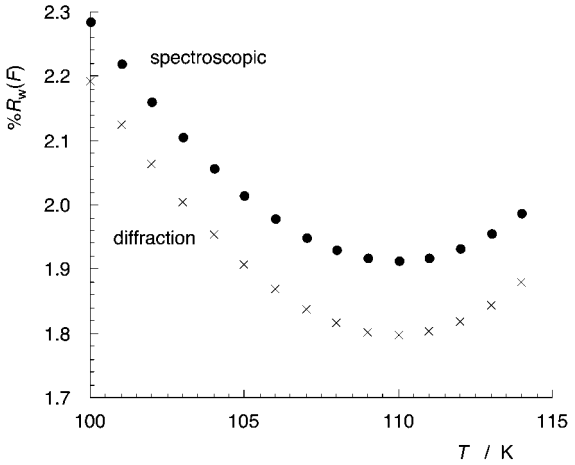

Figure 2. Weighted least-squares residual after multipole refinements A, plotted against temperature assumed in the calculation of C and H atom ADP's. The labels "diffraction" and "spectroscopic" indicate use of ADP's incorporating either of the two sets of intramolecular mean-square amplitudes, see Table 1.

consistently better ($R_w(F)$ 0.1 % lower) than those from spectroscopic ε's. Although the CCD X-ray data were nominally collected at 100 K, the differences between $R_w(F)$ at assumed T values of 100 K and 110 K in Figure 2 are substantial. From the static electron distributions derived in each of these multipole refinements, we have also computed values of the molecular quadrupole moment, Θ, the mean deuterium quadrupole coupling constant and the mean anisotropy of the EFG tensors at the H nuclei (see Results and Discussion for details), and these are plotted against assumed temperature in Figures 3, 4 and 5. In Figure 3 we see

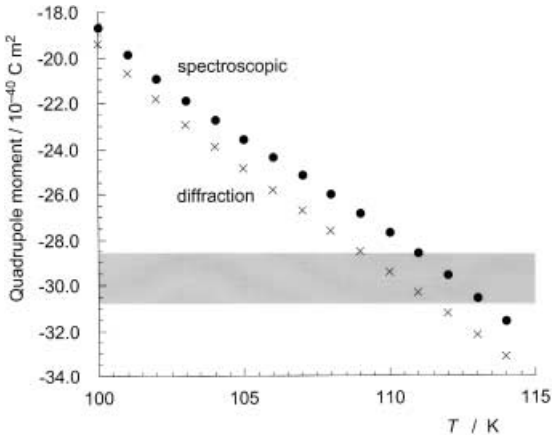

Figure 3. Molecular quadrupole moment, Θ, computed from total electron density, plotted against temperature assumed in the calculation of C- and H-atom ADP's. The shaded region is bounded by independent solution- and vapour-phase measurements of Θ.

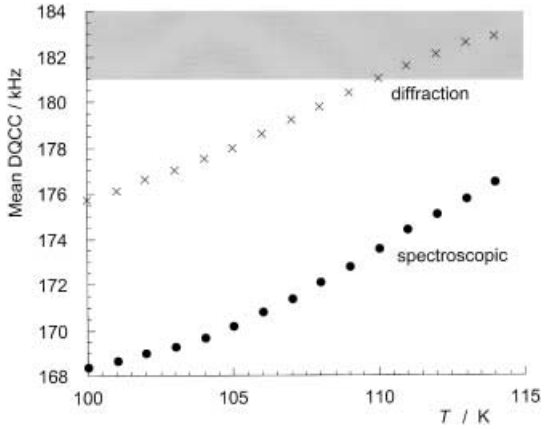

Figure 4. Deuterium quadrupole coupling constant computed from the average of $|\nabla E_{zz}|$ for the three H atoms, plotted against temperature assumed in the calculation of C- and H-atom ADP's. The shaded region indicates the lower bound of the range of independent measurements in the solid state (181 – 193 kHz).

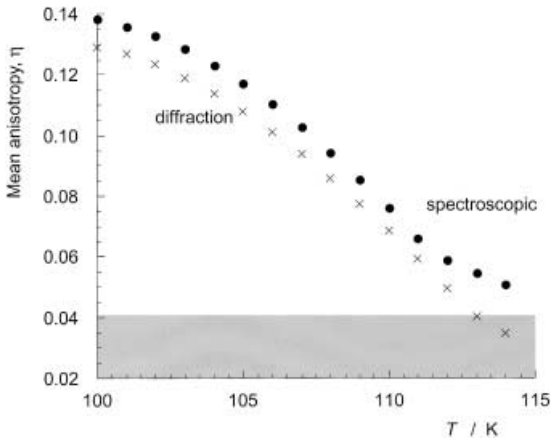

Figure 5. Mean anisotropy, η, of ∇E for the three H atoms, plotted against temperature assumed in the calculation of C-and H-atom ADP's. The shaded region indicates the range of values assumed or derived in independent studies of the solid state (0.0 – 0.041).

that, over the temperature range assumed, the derived quadrupole moment changes by a factor of two; only for $109\ \mathrm{K} < T < 113\ \mathrm{K}$ do the multipole-derived results lie within the range of values obtained from solution[23] or vapour-phase[24] measurements. Similarly, in Figure 4 the derived DQCC's are compared with the range of independent measurements obtained in the solid state (181–193 kHz, see Hardy et al.[25]). Only the "diffraction" results overlap the range of other values, and then only for $T \geq 110\ \mathrm{K}$. The mean anisotropy of the EFG tensor (Figure 5) suggests $T \geq 113\ \mathrm{K}$ but, as discussed below, the values plotted in Figure 5 are slightly compromized by the diagonalization procedure. The key observation from Figure 5 is that only for $T \gg 100\ \mathrm{K}$ do the EFG tensors at H nuclei approach their expected near-cylindrical symmetry (i.e. $\eta \approx 0$). All results presented in Figures 2–5 strongly suggest that the actual temperature of the CCD X-ray experiment was closer to 110 K than 100 K.

Table 2. Comparison of ADP's for C atoms in C_6H_6 obtained from models A (ADP analysis of neutron data on C_6D_6; assumed $T = 110$ K) and B (refined in the least-squares procedure). ADP's for H atoms obtained via ADP analysis at 110 K are also listed. For each atom, the upper triangle of the **U** tensor is given ($\times 10^4$ Å^2); least-squares standard errors in all values are less than 1 in the last figure.

	A						B					
atom	diffraction			spectroscopic			diffraction			spectroscopic		
C1	212	12	−12	213	14	−11	211	13	−7	211	13	−7
		181	−10		177	−9		186	−9		186	−9
			236			238			240			238
C2	197	13	29	195	14	33	195	13	27	195	13	27
		237	−18		237	−19		236	−17		236	−17
			221			220			222			222
C3	211	−21	10	211	−22	12	206	−17	11	206	−17	11
		215	20		213	22		215	18		215	18
			214			213			217			217
H1	478	85	17	495	93	29						
		260	8		256	12						
			533			550						
H2	402	81	177	413	88	195						
		489	−33		495	−32						
			458			471						
H3	471	−58	104	486	−57	119						
		398	125		400	135						
			433			445						

H atom ADP's as for A

The temperature at the nozzle blowing cold nitrogen gas onto the crystal was set at 100 K, but calibration against the phase transition of KH_2PO_4 (KDP) indicated that the temperature at the crystal position was 3 K higher than displayed on the controller. The CCD experiment was performed on a single crystal of benzene grown in situ in a capillary of diameter 0.5 mm (wall thickness 0.01 mm). The capillary dimensions correspond to a cross-section that is estimated to be about twice as large as that of the glass needle used to mount KDP. In addition, the length of the capillary mounted on a brass support was 10 mm, much larger than the diameter of the cold stream, which was about 3–4 mm. All of these considerations suggest two significant mechanisms for transferring heat to the benzene crystal, via the brass support and from the air via the capillary protruding beyond the N_2 stream, and on this basis the temperature at the crystal is estimated to be > 106 K. This is compatible with the above estimate of 110 K from the best R factor.

Results and Discussion

ADP's of carbon atoms at 110 K: All multipole refinements described above were obtained with model A: C and H atom ADP's were fixed at values obtained from the ADP analysis of C_6D_6 neutron data. For refinements with model B, we used H atom ADP's calculated by using an assumed temperature of 110 K, and varied C atom ADP's in the least-squares process. Table 2 reports ADP's of C and H atoms from both models A and B, and obtained with both diffraction and spectroscopic ε's. Carbon atom ADP's derived by thermal motion analysis of the C_6D_6 neutron data display virtually no difference with choice of diffraction or spectroscopic ε's, while H atom ADP's differ slightly, the spectroscopic ε's resulting in a greater ($\approx 2.2\,\%$) magnitude of thermal motion. The optimized values obtained from B:diff and B:spec refinements are indistinguishable from one another, and in exceptionally good agreement with the ADP's computed by ADP analysis at 110 K (see A:diff column). Considering the rather convoluted way in which these ADP's have been obtained (i.e. from the temperature dependence of neutron-derived ADP's on a different isotopomer, corrected for mass and temperature differences), and the extraordinary level of agreement between C-atom ADP's derived in this manner and those obtained from multipole refinement of the present CCD X-ray data, we feel confident that the H-atom ADP's presented in Table 2 accurately describe the nuclear motion of the protons in C_6H_6 at the temperature of the present X-ray experiment.

Refinement indices and the electron density: Table 3 reports refinement statistics and optimized radial parameters ob-

Table 3. Refinement statistics and optimized radial parameters.[a]

	A:diff	A:spec	B:diff	B:spec
% $R(F)$	2.01	2.15	1.89	1.89
% $R_w(F)$	1.80	1.91	1.68	1.69
% $R(F^2)$	2.32	2.45	2.27	2.28
% $R_w(F^2)$	3.83	4.10	3.60	3.60
GoF	1.10	1.17	1.04	1.04
κ_C	1.033(3)	1.038(3)	1.029(4)	1.028(4)
α_C [a.u.]	2.96(3)	3.06(3)	2.94(3)	2.94(3)
α_H [a.u.]	2.21(3)	2.25(3)	2.21(3)	2.23(3)

[a] $R(F) = \Sigma|\Delta|/\Sigma|F_o|$, $R_w(F) = [\Sigma w\Delta^2/\Sigma w|F_o|^2]^{1/2}$, and GoF $= [\Sigma w\Delta^2/(n_o - n_p)]^{1/2}$, in which $\Delta = |F_o| - |F_c|$ and the summation is over 1766 reflections with $F_o > 4\sigma(F_o)$. Expressions for $R(F^2)$ and $R_w(F^2)$ are obtained by substituting F^2 for $|F|$.

  0947-6539/02/0815-3516 $ 20.00+.50/0 *Chem. Eur. J.* **2002**, *8*, No. 15

tained in A:diff, A:spec, B:diff and B:spec refinements. All refinement indices support the conclusions from Figures 2–5, that B:diff represents a significantly better fit to the X-ray data. Moreover, we see that B:diff and B:spec refinements are virtually indistinguishable from one another, both showing significant improvements over the model A refinements, with $R_w(F)$ lowered by 0.12% in both cases.

Without going into great detail discussing electron density population parameters, we believe it is productive to provide some comparison between the values of α_C and α_H (Table 3) and other recent results. As expected from the previous discussion, values of these parameters differ little between refinements A:diff, B:diff and B:spec, and even the A:spec results are only marginally different. The C atom radial exponent obtained in refinements B, $\alpha_C = 2.94(3)$ a.u., agrees exceptionally well with the mean value of 2.92(6) a.u. obtained for a set of 27 sp^2 C atoms by Volkov et al.[26] in their recent and detailed analysis of multipole modelling of theoretical structure factors based on crystal density-functional calculations. Those workers also report exponents of H-atom radial functions, although the monopole and higher multipole exponents were optimized separately. For H bonded to C, Volkov et al. found that α_H clustered around 2.20 a.u. for monopole functions, and around 2.36 a.u. for higher multipoles. The present results (Table 3) are in excellent agreement with those outcomes.

The static deformation electron density in the molecular plane is shown in Figure 6. The contour interval of 0.05 eÅ^{-3} reflects the approximate experimental error in that map;

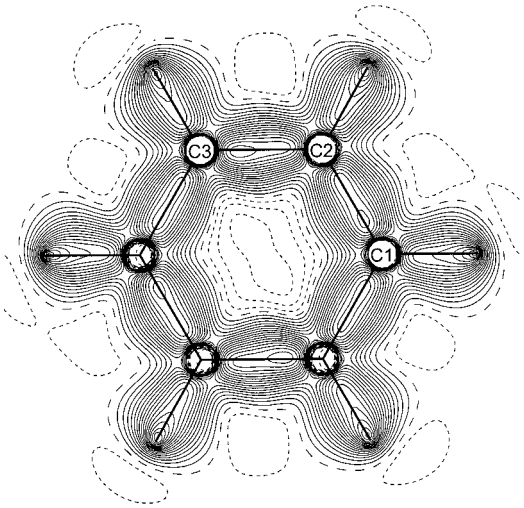

Figure 6. Static deformation electron density (multipole-derived electron density minus sum of spherical atoms) from B:diff refinement, in the molecular plane of benzene. Contours at 0.05 eÅ^{-3} intervals; positive contours solid, zero and negative contours dashed.

differences of one or two contours between chemically identical bonds are not likely to be significant. The C–H bonds are characterized by substantial build-up of electron density, reaching a peak of ≈0.90 eÅ^{-3} near the proton, but displaced towards the C atom in the bond; C–C bonds display quite flat regions peaking at ≈0.80 eÅ^{-3} along the C–C vector.

Molecular quadrupole moment: As discussed in some detail by Buckingham,[27] the distribution of electric charge in a molecule (i.e. both electrons and nuclei) is intimately related to its structure, and knowledge of the charge distribution sheds considerable insight into the molecule's reactivity and its interactions with other molecules. In particular, the electric multipole moments summarize the three-dimensional charge distribution, and can be used to determine the interaction energy of molecules at large separations. In his article of 1970 Buckingham even hinted at the possibility of extracting multipole moments from X-ray diffraction data. As described in the Introduction, the molecular quadrupole moment of benzene has been derived from the X-ray data of Jeffrey et al., and discussed in some detail by Spackman.[4] The value obtained was substantially greater than experimental or theoretical estimates, and that discrepancy provided some of the impetus for the present work.

Because benzene is such a highly symmetric molecule (point group D_{6h}), the molecular quadrupole moment tensor can be described by a single parameter, $\Theta_{zz} = -(\Theta_{xx} + \Theta_{yy})$, in which x and y are in the molecular plane, and z is perpendicular to the plane. However, in the solid state, the molecule possesses only an inversion centre (although it very closely approximates D_{6h} symmetry[2]), with the result that all five unique components of the traceless tensor may be nonzero. Because values for these tensor elements computed from a multipole refinement against X-ray data all contain inherent experimental errors, diagonalization of the tensor to produce something akin to Θ_{zz} is fraught with danger. To circumvent this problem we performed multipole refinements A and B using a coordinate system for the pseudoatom multipoles with one axis perpendicular to the mean molecular plane and the other two in the plane. In this manner, we obtained a meaningful quantity, the out-of-plane component of the quadrupole moment, which we denote by Θ, and which is directly comparable with independent experimental measurements.

Table 4 presents multipole-derived results for Θ, along with standard errors estimated from the covariance matrix at least-squares convergence. There are no significant differences between the multipole estimates of Θ, although in comparison with the results in Tables 2 and 3, it is clear that small differences in C- and/or H-atom ADP's have a marked effect on this quantity. The most important outcome from Table 4 is

Table 4. Comparison between molecular quadrupole moments of benzene derived from present multipole refinements and independent experimental measurements.

	Θ [10^{-40} C m^2]
multipole derived	
A:diff	-29.4 ± 2.5
A:spec	-27.7 ± 2.6
B:diff	-29.7 ± 2.4
B:spec	-28.7 ± 2.4
dilute solution[a]	-28.3 ± 1.2
vapour phase[b]	-30.4 ± 1.2

[a] Mean of six independent determinations by field-gradient-induced birefringence on dilute solutions of benzene in carbon tetrachloride.[23] [b] Derived from temperature dependence of the field-gradient birefringence on benzene vapour.[24]

that all multipole-derived estimates of the molecular quadrupole moment in benzene (i.e. in the solid state) are of the same sign as, and lie near to or between, independent measurements obtained in the gas phase and in dilute solution. A negative sign implies a ring of positive charge in the molecular plane near the hydrogen atoms, with negative regions above and below the 6-ring. The present estimates are entirely consistent with the expectation that the weak intermolecular forces present between benzene molecules have a very small, and presently unobservable, effect on the molecular quadrupole moment.

Electric field gradients at protons and deuterium quadrupole coupling constants: These quantities have been described in a preliminary fashion in the Introduction, but it is essential to provide additional background and details of the computation procedure in order to best understand the outcomes. Stewart[28] first suggested the estimation of EFG tensors from multipole refinement results in 1972, and a limited number of attempts have been made since that time; Brown and Spackman[8] provided a summary up to 1994. Brown and Spackman also summarized four computational strategies that may be used to derive EFG tensors from multipole-derived electron densities; in the present work all results have been computed by direct space summation over the crystal, including contributions from all pseudoatoms within a 5 Å sphere of each proton.

Our focus in this work is on the EFG's at H-atom positions, and it is worth emphasizing that hydrogen is unique with respect to the determination of EFG tensors from multipole-derived electron distributions. Because of the lack of core electrons, the EFG at the hydrogen nucleus has two main contributions: the electron distribution of nearest-neighbour atoms (which is dominated by the monopole term on the atom bonded to hydrogen), and the valence quadrupole deformation at the H atom. Core deformation, which is present in all other atoms and which manifests itself as sharp deformations close to the nucleus, is difficult to determine from X-ray diffraction data, even from data of the quality and resolution reported in this work. In the presence of core deformations, satisfactory EFG tensors can only be obtained by addition of empirical correction factors (see for example the recent work on aluminosilicate polymorphs[29]). Tegenfeldt and Hermansson[30] first reported DQCC's derived from experimental electron distributions by a combined direct- and reciprocal-space strategy, although the coupling constants they obtained are substantially larger than nuclear quadrupole resonance (NQR) results (by more than 100 kHz in some cases), which precluded any quantitative comparisons.

The components of the EFG tensor at $\mathbf{r}'$ are the second derivatives of the electrostatic potential $\phi(\mathbf{r})$, for example $\nabla E_{xy}(\mathbf{r}')$ in Equation (4):

$$\nabla E_{xy}(\mathbf{r}') = -\left(\frac{\partial^2\phi(\mathbf{r})}{\partial x \partial y}\right)_{\mathbf{r}=\mathbf{r}'} \quad (4)$$

∇E is conventionally cast in traceless form when describing its interaction with a nuclear quadrupole moment, and we assume this form in the present work. The principal axes of the tensor are conventionally labelled such that $|\nabla E_{zz}| \geq |\nabla E_{yy}| \geq |\nabla E_{xx}|$, here x, y and z refer to the principal directions (i.e. following diagonalization of the tensor). The quantities most commonly used to describe the EFG tensor in crystals are ∇E_{zz}, the asymmetry parameter, $\eta = (\nabla E_{xx} - \nabla E_{yy})/\nabla E_{zz}$, which describes the deviation of the EFG tensor from axial symmetry, and the orientation of the principal axes with respect to the crystallographic axes. Experimental studies also frequently cite the quadrupole coupling constant, $-eQ\nabla E_{zz}/h$, in which Q is the nuclear quadrupole moment. The relationship between multipole-derived EFG results and deuterium quadrupole coupling constants (DQCC's) can be expressed in the form[8] DQCC/kHz $= 99.6(5) \times (-\nabla E_{zz}/$ eÅ^{-3}).

Our interest in the present study is not just the DQCC's derived from EFG tensors at each proton, but also the shape and orientation of the tensors. As described above for the quadrupole moment, each component of the EFG tensor computed from multipole refinement results has an associated experimental error, and this introduces considerable error into the diagonalization procedure. As for Θ, we choose a cartesian-coordinate system for the calculation of EFG tensor components, in this case the natural one suggested by the bonding environment of each H atom in benzene and the principal axes of the inertia tensor of the molecule, namely along the C–H bond (∇E_{11}), in the molecular plane (∇E_{22}), and perpendicular to the molecular plane (∇E_{33}). (As these directions are identical to those used earlier in the description of ε tensors, we label them in an identical fashion). In this frame, the off-diagonal components of the EFG tensors are not zero, but are uniformly small. We have not performed a detailed error analysis on these results, as the computation of standard errors for EFG's from the least squares covariance matrix has not yet been implemented in VALRAY. Table 5 summarizes EFG results for the four refinements already

Table 5. Components of EFG tensors (eÅ^{-3}), implied deuterium quadrupole coupling constants, DQCC (in kHz) and tensor asymmetries, η, for the three H atoms in benzene.[a]

		A:diff	A:spec	B:diff	B:spec
H1	∇E_{11}	−1.751	−1.676	−1.742	−1.701
	∇E_{22}	0.838	0.786	0.836	0.833
	∇E_{33}	0.913	0.889	0.906	0.868
	η	0.043	0.062	0.040	0.020
	DQCC	174.4	166.9	173.5	169.4
H2	∇E_{11}	−1.967	−1.891	−2.000	−1.966
	∇E_{22}	0.915	0.884	0.914	0.917
	∇E_{33}	1.052	1.007	1.087	1.050
	η	0.070	0.065	0.087	0.068
	DQCC	195.9	188.3	199.2	195.8
H3	∇E_{11}	−1.714	−1.638	−1.753	−1.714
	∇E_{22}	0.824	0.802	0.830	0.828
	∇E_{33}	0.890	0.836	0.923	0.886
	η	0.039	0.021	0.054	0.033
	DQCC	170.7	163.1	174.6	170.7
mean	DQCC[b]	180 ± 16	173 ± 15	182 ± 17	179 ± 17
mean	η[b]	0.051 ± 0.019	0.049 ± 0.028	0.060 ± 0.027	0.040 ± 0.028

[a] EFG tensors are reported with respect to local axes on each atom: ∇E_{11} is along the C–H bond; ∇E_{22} is in plane and perpendicular to the C–H bond; ∇E_{33} is perpendicular to the molecular plane. Off-diagonal components are not zero, but are small in all cases (absolute value less than 0.07 eÅ^{-3}). [b] Reported errors are maximum deviations from the mean.

0947-6539/02/0815-3518 $ 20.00+.50/0 *Chem. Eur. J.* **2002**, *8*, No. 15

considered, and several important conclusions emerge from these results.

For all refinements the tensor components satisfy $|\nabla E_{11}| > |\nabla E_{33}| > |\nabla E_{22}|$; this is at variance with the assignment based on high-resolution rotational spectroscopy of monodeuterobenzene[31] (for which $|\nabla E_{33}| < |\nabla E_{22}|$), but in agreement with recent density-functional calculations on benzene at the B3LYP/6–31G(*df*,3*p*) level.[32] As discussed by Bailey, it appears that the experimental tensor components *bb* and *cc* (i.e. those corresponding to the smallest two rotational constants) were incorrectly assigned, and this is supported by similar experimental results for 4-fluoro-1-deuterobenzene.[31] The EFG tensor anisotropy, η, is highly sensitive to small changes in the three components, largely because ∇E_{22} and ∇E_{33} differ by only a small amount ($\approx 10\,\%$), but all results lie in the range 0.020–0.087 in agreement with the expectation of nearly axial symmetry. This is a result of some importance, as the multipole models imposed no local symmetry on the C or H atoms in the crystal. Obtaining EFG asymmetry parameters of the correct magnitude for H atoms provides strong confirmation that the CCD X-ray data, the electron density model and, especially, the description of H-atom vibrational motion (i.e. ADP's) contain no substantial systematic errors.

The DQCC is readily derived from ∇E_{11}. For all refinements the DQCC implied by the EFG at H2 is significantly larger (by 20–25 kHz) than those at H1 and H3, which are essentially the same. This outcome is so robust and independent of the vibrational motion model chosen that we tentatively ascribe it to the effect of the weak C–H$\cdots\pi$ interaction which is experienced by H2 (see Figure 1), and not by either of H1 or H3. From the neutron structure at 15 K,[2] H1 makes close contacts to four other H atoms (range 2.60–2.68 Å) and to C3 (2.88 Å), H3 is close to three H atoms (range 2.50–2.68 Å) and to C1 (2.86 Å), while H2 is close to only two H atoms (range 2.50–2.60 Å), but is directly above the benzene ring and 2.75 Å from its centre (the ring C atoms are all within 3.06–3.10 Å).

It is clear from Table 5 that A:diff, B:diff and B:spec refinements yield essentially identical mean DQCC's, while the value emerging from A:spec is somewhat lower. This trend is similar to that observed above for ADP's and for the molecular quadrupole moment, and it lends further support to the expectation that the B:diff results are probably the most reliable of those from the present study. Hardy and coworkers[25] have summarized literature results for DQCC's in benzene-related species, in the gas phase, in neat solutions, in nematic solutions and in polycrystalline and single-crystal specimens. As summarized in that work, all reliable data lie in the range 181–193 kHz and, within the uncertainties reported for those measurements, a difference between the phases cannot be detected. The best of the present results lie at the lower end of this range, and it is informative to explore this in further detail.

We focus on results from polycrystalline and single crystal samples. Rowell et al.[33] measured quadrupole splittings in deuteron magnetic resonance (DMR) spectra on a polycrystalline sample of C_6D_6 over 14 different temperatures (109 K to room temperature), and reported an average DQCC of 193 ± 3 kHz; an asymmetry parameter of zero was assumed. Barnes and Bloom[34] fitted both the DQCC and η to DMR line shapes derived from polycrystalline samples of benzene at 77 K, obtaining 180.7 ± 1.5 kHz and $\eta = 0.041 \pm 0.007$ for C_6D_6 and 176.7 ± 1.5 kHz and $\eta = 0.053 \pm 0.005$ for naphthalene, $C_{10}D_8$. More recently Ok et al.[35] used DMR methods to study molecular motion of C_6D_6 in a 1,3-cyclohexanedione cyclamer and in solid C_6D_6. For the pure solid at temperatures between 87 K and 130 K, a DQCC of 183 ± 1 kHz was obtained, with $\eta = 0.040 \pm 0.005$. Of these measurements on polycrystalline samples, the most recent are in excellent agreement with the present multipole-derived values. To our knowledge, the only DMR experiment performed on a C_6D_6 single crystal is that reported by Pyykkö and Lähteenmäki at 263 K.[36] At this temperature hindered rotation is still quite fast, and the DQCC derived from an analysis of the 180° DMR rotation pattern is actually that corresponding to ∇E_{33}. The result of 93.3 ± 0.8 kHz (see Table 1 of that work) can be used to derive a DQCC corresponding to ∇E_{11} provided a value of η is known or assumed. Pyykkö and Lähteenmäki assumed $\eta = 0$ and obtained a DQCC of 186.6 ± 1.6 kHz. However, if we assume $\eta = 0.041 \pm 0.007$ as obtained by Barnes and Bloom, we obtain a DQCC of 179.3 ± 2.8 kHz. This modified result is in exceptionally good agreement with the A:diff, B:diff and B:spec results in Table 5.

Conclusion

This charge density study on benzene set out to establish whether, with highly accurate X-ray diffraction data, it was possible to derive physical properties for benzene that compare quantitatively with other experimental measurements. We believe we have demonstrated conclusively that this is the case for the molecular quadrupole moment of benzene and for the EFG's at the H nuclei, and summarize our conclusions as follows:

- The multipole-derived estimates of the molecular quadrupole moment of benzene lie near or between measurements on dilute solutions and the vapour, and support the expectation that this property is not significantly affected by the weak intermolecular forces.
- The mean multipole-derived DQQC's are in excellent agreement with NQR experiments on single crystal and polycrystalline samples of C_6D_6. However, the multipole refinement yields full information on the EFG tensor and, most importantly, provides information on each symmetry-unique H atom. In the present case, the diffraction data and modelling procedure suggest that the EFG and DQCC at H2 are significantly different from those at H1 and H3; we tentatively ascribe this to the different environments in the crystal, and possibly the participation of H2 in a C–H$\cdots\pi$ interaction in the solid.
- The ADP analysis pursued in this work in order to accurately describe the vibrational motion of the atomic nuclei, especially protons, was vital to obtaining successful outcomes. The procedure described by Bürgi and coworkers is clearly enormously powerful, and deserves to be pursued with enthusiasm by charge-density workers. Multi-

temperature X-ray data combined with spectroscopic or ab initio force fields should be capable of providing ADP's for H atoms, and this will enable more accurate electron density modelling, especially for H atoms. Approaches in this direction, with ab initio or spectroscopic force fields and molecular rigid-body librations derived from refined ADP's for heavy atoms, have already been employed by Koritsanszky and co-workers,[37–39] and by Destro and co-workers.[40, 41] It is probably not a coincidence that the only other experimental charge density study which yields DQCC's in quantitative agreement with NMR experiments was that by Destro et al. on α-glycine.[40]

- CCD X-ray diffraction data, even for crystals grown in situ in capillaries, can be of very high quality. Together with improved models of motion, they promise to provide charge density quality data sets that are increasingly accurate and precise. They are measured in a fraction of the time taken by conventional diffractometers and point detectors; this presents a considerable challenge to the methods of analysing the data for the extraction of chemical and physical information.

Experimental Section

A single crystal of benzene was grown in a glass capillary ($\varnothing = 0.5$ mm) mounted on the goniometer of a Bruker SMART CCD 1 K diffractometer equipped with an Oxford Cryostream N_2 LT-device.[42] A polycrystalline sample was obtained on cooling to 250 K, which was then warmed to 275 K until just a tiny crystalline seed remained in the very tip of the capillary. Slow cooling of the seed to 272 K produced a crystal of suitable quality and about 5 mm long, i.e. longer than both the diameter of the X-ray beam and the nitrogen cold stream (3–4 mm). The crystal was then cooled further to the temperature of the data collection.

The faceplate of the CCD detector was positioned at 4.5 cm from the optical centre of the goniometer. Measurements were made at a temperature, as indicated by the cryostat's controller, of 100.0(2) K with the detector at two different positions of $2\theta = -29^\circ$ and -78°; five positions of the ϕ axis at each detector position, and 20 and 40 s exposures respectively. A total of 6220 frames was collected using ω scans (0.25°/frame) and processed with SAINT,[43] blending the model peak profiles of the reflections from different detector regions (option BLEND). Because peak profiles were far from ideal, the integration-box size recommended by SAINT was not used. Instead, the box size was selected in order to obtain reasonable (<10%) values of maximum profile on the box boundaries, resulting in $x = y = 3.8$, $z = 1.2$, a box size somewhat larger than used for standard high-quality crystals. Data were corrected for systematic errors and absorption effects using SADABS,[44] minimum effective transmission 0.620 (preliminary calculations indicate that this ratio of minimum to maximum transmission factor is due largely to the change of the irradiated crystal volume associated with the change in orientation of the capillary relative to the X-ray beam). Merging of the corrected data was performed with zero-weighting of outliers (655 in total) with $I - I_{mean} \geq 6\sigma(I)$, by using the SORTAV program of the DREAD package.[45] Crystal data and some details of data collection and refinement are given in Table 6.

Although all refinements and results reported in the present work are based upon the data set summarized in Table 6, two further reduced data sets were obtained from the same raw data by using different integration-box sizes. To our knowledge, this influence of integration-box size on derived structural, thermal and electron-density parameters has not been adequately explored to date, and the present modest attempt serves to further validate the results already presented above. Smaller ($x = y = 1.9$, $z = 1.0$) and larger ($x = y = 5.0$, $z = 2.0$) box sizes were chosen, resulting in R_{merge} values of 2.34% and 3.36%, respectively, compared with 2.58% for the original data (Table 6). The smaller box size showed rather high values of maximum profile on the box boundary, especially for high-angle data.

Table 6. Crystal data and structure refinement for benzene

empirical formula	C_6H_6
formula weight [g mol^{-1}]	312.43
crystal system	orthorhombic
space group	P*bca*
Z	4
temperature [K]	100
a [Å]	6.7809(2)
b [Å]	7.4093(2)
c [Å]	9.4541(3)
$\alpha = \beta = \gamma$ [°]	90.0
V [Å^3]	474.99(4)
calculated density [g cm^{-3}]	1.091
$F(000)$	168.0
absorption coefficient μ [mm^{-1}]	0.06
λ [Å]	0.71073
$(\sin\theta/\lambda)_{max}$ [Å^{-1}]	1.11
limiting indices	$-15 \leq h \leq 14$, $-16 \leq k \leq 16$, $-20 \leq l \leq 20$
number of frames collected	6220
number of reflections measured	20 741
symmetry independent reflections	2718
completeness	98.9%
R_{int} [a]	0.0258
R_{int} (for $I \geq 2\sigma(I)$)	0.0225

[a] $R_{int} = \Sigma | F_o^2 - F_o^2(\text{mean}) | / \Sigma F_o^2$.

Both additional data sets were subjected to the same refinement strategies described earlier (i.e. both models A and B). In all cases, the original data set yielded R values consistently lower than those obtained from the smaller box size (for model A, 1.80% vs. 1.99%), and substantially lower than those obtained with the larger box size (3.61% for model A). "Optimum" temperatures derived from model A refinements were 112 K (smaller box size) and 106 K (larger box size), which bracket the result of 110 K from the original data (Figure 2). Derived quadrupole moments and DQCC's from these alternative data sets also bracket the results reported earlier from the original data, the quadrupole moment being especially sensitive to choice of box size. In conclusion, it would seem that the original, carefully chosen, box size is somewhat optimal, being a balance between a choice that is unreasonably small and truncates a significant number of reflection profiles, and one that incorporates too much background and results in markedly inferior merging statistics and refinement results.

Acknowledgements

We thank the Australian Research Council and the Schweizerischer Nationalfonds for financial support, and Birger Dittrich (Free University of Berlin) for producing Figure 1.

[1] G. A. Jeffrey, C. W. Lehmann, J. R. Ruble, Y. Yeon, *unpublished results*, **1989**.
[2] G. A. Jeffrey, J. R. Ruble, R. K. McMullan, J. A. Pople, *Proc. R. Soc. London Ser. A* **1987**, *414*, 47–57.
[3] R. F. Stewart in *The Application of Charge Density Research to Chemistry and Drug Design* (Eds.: G. A. Jeffrey, J. F. Piniella), Plenum Press, New York, **1991**, pp. 63–102.
[4] M. A. Spackman, *Chem. Rev.* **1992**, *92*, 1769–1797.
[5] Z. Su, P. Coppens, *Acta Crystallogr. Sect. A* **1992**, *48*, 188–197.
[6] Z. Su, P. Coppens, *Z. Naturforsch.* **1993**, *48a*, 85–90.
[7] Z. Su, *J. Comput. Chem.* **1993**, *14*, 1036–1041.
[8] A. S. Brown, M. A. Spackman, *Mol. Phys.* **1994**, *83*, 551–566.
[9] A. E. Goeta, PhD thesis, Universidad Nacional de La Plata (Argentina) **1995**.
[10] C. Flensburg, PhD thesis, University of Copenhagen (Denmark) **1999**.
[11] R. H. Blessing, *Acta Crystallogr. Sect. B* **1995**, *51*, 816–823.

  0947-6539/02/0815-3520 $ 20.00+.50/0

[12] R. K. McMullan, T. F. Koetzle, C. J. Fritchie, *Acta Crystallogr. Sect. B* **1997**, *53*, 645–653.
[13] H. B. Bürgi, S. C. Capelli, *Acta Crystallogr. Sect. A* **2000**, *56*, 403–412.
[14] V. Schomaker, K. N. Trueblood, *Acta Crystallogr. Sect. B* **1968**, *24*, 63–76.
[15] E. B. Wilson, J. C. Decius, P. C. Cross, *Molecular Vibrations*, McGraw-Hill, New York, **1955**.
[16] S. C. Capelli, M. Förtsch, H. B. Bürgi, *Acta Crystallogr. Sect. A* **2000**, *56*, 413–424.
[17] L. Goodman, A. G. Ozkabak, S. N. Thakur, *J. Phys Chem.* **1991**, *95*, 9044–9058.
[18] P. Coppens, *X-Ray Charge Densities and Chemical Bonding*, Oxford University Press, New York, **1997**.
[19] C. Flensburg, S. Larsen, R. F. Stewart, *J. Phys Chem.* **1995**, *99*, 10130–10141.
[20] R. F. Stewart in *Electron and Magnetization Densities in Molecules and Solids* (Ed.: P. Becker), Plenum, New York, **1980**, pp. 427–431.
[21] E. Clementi, C. Roetti, *At. Data Nucl. Data Tables* **1974**, *14*, 177–478.
[22] R. F. Stewart, M. A. Spackman, VALRAY Users Manual, Chemistry Department, Carnegie-Mellon University, **1983**.
[23] G. R. Dennis, G. L. D. Ritchie, *J. Phys Chem.* **1991**, *95*, 656–660.
[24] G. L. D. Ritchie, J. N. Watson, *Chem. Phys. Lett.* **2000**, *322*, 143–148.
[25] E. H. Hardy, R. Witt, A. Dölle, M. D. Zeidler, *J. Mag. Res.* **1998**, *134*, 300–307.
[26] A. Volkov, Y. A. Abramov, P. Coppens, *Acta Crystallogr. Sect. A* **2001**, *57*, 272–282.
[27] A. D. Buckingham in *Physical Chemistry. An Advanced Treatise* (Ed.: D. Henderson), Academic Press, New York, **1970**, pp. 349–386.
[28] R. F. Stewart, *J. Chem. Phys.* **1972**, *57*, 1664–1668.
[29] S. Dahaoui, N. E. Ghermani, S. Ghose, J. A. K. Howard, *Am. Mineral.* **2000**, *86*, 159–164.
[30] J. Tegenfeldt, K. Hermansson, *Chem. Phys. Lett.* **1985**, *118*, 293–298.
[31] S. Jans-Bürli, M. Oldani, A. Bauder, *Mol. Phys.* **1989**, *68*, 1111–1123.
[32] W. C. Bailey, *J. Mol. Spec.* **1998**, *190*, 318–323.
[33] J. C. Rowell, W. D. Phillips, L. R. Melby, M. Panar, *J. Chem. Phys.* **1965**, *43*, 3442–3454.
[34] R. G. Barnes, J. W. Bloom, *J. Chem. Phys.* **1972**, *57*, 3082–3086.
[35] J. H. Ok, R. R. Vold, R. L. Vold, M. C. Etter, *J. Phys Chem.* **1989**, *93*, 7618–7624.
[36] P. Pyykkö, U. Lähteenmäki, *Ann. Univ. Turku A* **1966**, *93*, 2–7.
[37] J. Buschmann, T. Koritsanszky, D. Lentz, P. Luger, N. Nickelt, S. Willemsen, *Z. Kristallogr.* **2000**, *215*, 487–494.
[38] R. Flaig, T. Koritsanszky, D. Zobel, P. Luger, *J. Am. Chem. Soc.* **1998**, *120*, 2227–2238.
[39] T. Koritsanszky, J. Buschmann, D. Lentz, P. Luger, G. Perpetuo, M. Röttger, *Chem. Eur. J.* **1999**, *5*, 3413–3420.
[40] R. Destro, P. Roversi, M. Barzaghi, R. E. Marsh, *J. Phys. Chem. A* **2000**, *104*, 1047–1054.
[41] P. Roversi, M. Barzaghi, F. Merati, R. Destro, *Can. J. Chem.* **1996**, *74*, 1145–1161.
[42] J. Cosier, A. M. Glazer, *J. Appl. Cryst.* **1986**, *19*, 105.
[43] SAINT, Version 5.00, Bruker AXS, Madison, WI (USA) **1998**.
[44] G. M. Sheldrick, SADABS: Program for scaling and corrections of area-detector data, University of Göttingen, Germany, **1996**.
[45] R. H. Blessing, *J. Appl. Cryst.* **1997**, *30*, 421–426.
[46] S. C. Capelli, PhD Thesis, University of Bern, Switzerland, **1999**.
[47] E. Keller, SCHAKAL97, University of Freiburg, Germany, **1997**.

Received: January 29, 2002 [F3834]